ACTA PHYSICA POLONICA A No. 4 Vol. **141** (2022)

Proceedings of the International Conference on Oxide Materials for Electronic Engineering (OMEE 2021)

Modification of Electrophysical Properties of Dense Anodic Alumina by Surfactant Addition to Anodizing Electrolyte

V. Shulgov*

Belarusian State University of Informatics and Radioelectronics (BSUIR),
6 Brovka Str., 220013 Minsk, Belarus

Doi: 10.12693/APhysPolA.141.298

*e-mail: shulgov@bsuir.by

The oxidation kinetics and chemical composition of dense anodic alumina obtained in electrolytes with surfactant additives were studied. Organic compounds from the class of alcohols were used as surfactants. Experimental data on the effect of surfactants on the anodic oxidation kinetics of aluminum were obtained by taking polarization curves. The chemical composition of the films was studied by the SIMS method. The surfactant introduction into the anodizing electrolyte has been shown to increase the insulation resistance and breakdown voltage of the films obtained due to the reduction of the number of hydroxide ions injected into the oxide film from the electrolyte.

topics: aluminum anodization, electrolyte, surfactant, dense anodic alumina

1. Introduction

In the process of aluminum electrochemical anodizing, dense (barrier) and/or porous alumina films can be formed, depending on the electrolyte composition. Dense (barrier-type) oxide films are formed when aluminum is anodized in neutral solutions (pH = 5–7), which negligibly dissolve aluminum oxide.

Dense anodic alumina films up to 1000 nm thick can be used as a dielectric layer in thin-film capacitors, inter-element and inter-level insulating layers in a multilevel interconnection system as well as the top protective layer of the passive part of hybrid integrated circuits, etc. [1–5]. To date, the studies on the formation of dense anodic alumina films and their behavior have been the subject of an extensive literature. However, the variety of functional capabilities of dense oxides in microelectronic technology, the specificity of microminiaturization problems, and increased requirements for the reliability of devices necessitate a deeper and more detailed knowledge of the features of anodic aluminum oxide.

The properties of dense anodic oxide films can be modified by changing the concentration and depth of penetration of electrolyte anions introduced into the growing anodic oxide film during anodizing, as well as the width of the homogeneous aluminum oxide zone. All of this makes it possible to change the composition and structure of dense aluminum oxides, which undoubtedly leads to a change in their electrophysical properties. The introduction of electrolyte anions into the oxide is strongly conditioned by the composition of anodizing electrolytes. The use of surfactants as additives to conventional electrolytes is one of the ways of influencing the anodizing process and oxide properties. The effect of surfactants should primarily appear during the process of ionic transfer at the oxide-electrolyte boundary and change the anionic composition of the surface layer of the oxide. Their influence on the double electric layer structure of the electrode-solution interface is well known [6, 7]. The present work is focused on the kinetics of aluminum anodic oxidation in the presence of surfactant additives for the formation of dense alumina films and their influence on the electrophysical properties of the oxides.

2. Experimental

The effect of surfactants on the oxidation kinetics of aluminum at the initial stages of the anodizing voltage sweep (0–10 V) was studied on films obtained by the electron-beam sputtering of A99 aluminum on an ST-50 citallic substrate of size 60×48 mm. The parameters of the sputtering modes were as follows: vacuum in the chamber was $6\text{–}7 \times 10^{-4}$ Pa; the substrate temperature was 393 K; the deposition rate was 4–5 nm/s; the film thickness was 1.5 μm. After sputtering, the substrates were divided into 10×48 mm^2 areas by scribing. Anodization areas of 100 mm^2 were formed on the surface of the aluminum film by photolithography. In further electrochemical measurements, the electrolyte-air interface was isolated from the

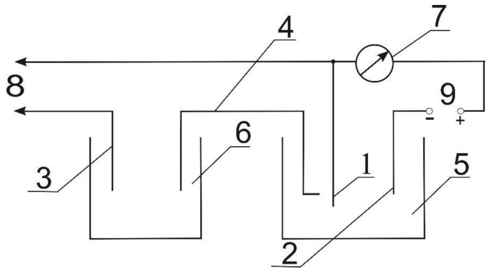

Fig. 1. Block diagram of the setup for measuring polarization curves: 1 — investigated electrode; 2 — auxiliary electrode; 3 — reference electrode; 4 — electrolytic key; 5 — vessel with electrolyte; 6 — a vessel with a supersaturated KCl solution; 7 — ammeter; 8 — high-resistance voltmeter; 9 — power supply.

surface of the metal film by a photo-resist layer, which made it possible to exclude the influence of meniscus processes from the consideration.

The effect of surfactants on the oxidation kinetics and properties of dense anodic alumina films was studied using the 1% aqueous citric acid solution (electrolyte A) as a background electrolyte during aluminum anodizing. The following organic compounds from the alcohol class were used as surfactants, i.e., triethanolamine $(HOCH_2CH_2)_3N$ (electrolyte B), glycerin $(CH_2OH)_2CHOH$ (electrolyte C), ethylene glycol $C_2H_2(OH)_2$ (electrolyte D), isopropyl alcohol $(CH_3)CHOH$ (electrolyte E), and ethyl alcohol C_2H_5OH (electrolyte F). The initial substances were at least of "pure to analysis" purity grade. The choice of additives is based on the following considerations. Alcohols dissolve well in water forming homogeneous solutions over large concentration ranges. In addition, the processes of alcohol absorption in aqueous solutions by the metal surface are well studied and their quantitative characteristics are available. According to existing concepts, alcohols are related to non-ionogenic surfactants, and this may have a significant impact on the structure and composition of anodic oxides. In addition, there are data on the successful practical use of alcohol additives in electrolytes for anodizing aluminum and its alloys [8–9].

Experimental data on the influence of surfactants on the anodic aluminum oxidation kinetics were obtained by taking polarization curves [10]. This method is one of the stationary methods for studying the electrode processes and allows to obtain the relationship between the anode current i_a and the anode potential ϕ_a. The block diagram of the unit for taking polarization curves (direct potentiostatic method) is shown in Fig. 1 [10].

The voltage source 9 is used to set a certain potential value of the studied electrode, relative to the reference electrode. The values of the anode current are recorded by ammeter 7 in series.

When measuring the polarization curves, a standard silver-chloride electrode placed in a supersaturated potassium chloride solution was used as a reference electrode. Its potential under these conditions is −1.56 V. The capillary tip of the electrochemical switch was placed as close as possible to the surface of the sample so that the measured electrode potential values would not be affected by the voltage drop in the solution.

The growth of dense anodic alumina films was studied with a linear sweep of the anodizing voltage at a rate of $15–20 \times 10^{-3}$ V/s in the anode potential range from 0 to 80 V. Then the voltage source was automatically switched to the constant voltage mode. The sweep rate of 1 V/s, which is most widely used in the anodizing technique, does not allow for a detailed study of the oxidation kinetics, especially in the initial stages of growth.

The surfactant concentration in the background electrolyte varied from 0.1 to 1 M. The electrolytes were prepared by dissolving the calculated amount of additive in half of the required electrolyte volume and then adjusting to the desired level by adding the background solution followed by careful stirring. The electrolyte compositions are presented in Table I. For example, electrolyte $B_{0.1\ \mathrm{M}}$ is a mixture of a 0.1 molar solution of triethanolamine and a 1% aqueous solution of citric acid.

The chemical composition of the anodic aluminum oxide films was studied by the SIMS method using the TOF.SIMS 5 unit (IONTOF; Munster, Germany). The sample was sputtered by a focused ion beam of Cs^+ ions with 2 keV energy and a raster on the sample surface of 150 μm^2. For this study, 0.75 μm thick aluminum films were deposited by the electron-beam evaporation onto the silicon substrates using the same regimes as those used for the citallic substrates. The substrates were then divided into 10×30 mm^2 areas by scribing. Then, dense anodizing of aluminum films in $D_{0.5\ \mathrm{M}}$ electrolyte was performed. The initial current density was 5 mA/cm^2. The cell voltage increased linearly with time at a rate of 0.1 V/s, and when it reached 200 V, the voltage source automatically switched to the constant voltage mode. The current density decreased exponentially over time. After 20 min, the residual currents were measured. They were 32 mA for anodizing in background electrolyte A and 21 mA for anodizing in electrolyte $D_{0.5\ \mathrm{M}}$, respectively. These samples were then subjected to SIMS analysis.

Contacting device with a mercury electrode was used to measure the electrophysical parameters of the anodic alumina films (see Fig. 2), using the following method. A fluoroplastic cylinder (4) was placed on the surface of the studied anodic aluminum oxide film (3). A drop of mercury (5) was placed in the cylinder, and the electrode (6) was immersed in the mercury drop. The second electrode (7) was placed on the surface of the sample

TABLE I

Characteristics of polarization curves in the studied electrolytes. Here, ϕ_{br} [V] is the anode potential, at which a significant increase in the current is observed; i_{br} [mA] is the anode current at the corresponding values of ϕ_{br}; ϕ_1 [V] is the anode potential, at which the first peak of the anode current is observed; i_{a1} [mA] is the anode current corresponding to the potential ϕ_1; $\phi_{\max}$ [V] is the anode potential, at which the maximum current is observed; $i_{\max}$ [mA] is the maximum current; ϕ_{st1}, ϕ_{st2} [V] are the anode potentials at which the anode current remains steady; i_{st} [mA] is the steady-state current; and i_{res} [mA] is the residual anode current after 10 min of the potentiostatic anodizing.

Electrolyte type	ϕ_{br} [V]	i_{br} [mA]	ϕ_{br} [V]	i_{a1} [mA]	$\phi_{\max}$ [V]	$i_{\max}$ [mA]	ϕ_{st1} [V]	ϕ_{st2} [V]	i_{st} [mA]	i_{res} [mA]
A	0.3	0.3	5.5	0.75	23	1.36	40	70	0.39	0.03
$\mathrm{B}_{0.1\ \mathrm{M}}$	0.5	0.2	5.0	0.5	–	–	20	75	0.39	0.02
$\mathrm{B}_{0.5\ \mathrm{M}}$	0.5	0.5	3.0	0.51	–	–	20	70	0.3	0.02
$\mathrm{B}_{1\ \mathrm{M}}$	–	–	7.0	1.5	–	–	16	80	0.39	0.03
$\mathrm{B}_{0.1\ \mathrm{M}}$	0.4	0.22	3.1	0.4	–	–	25	75	0.38	0.02
$\mathrm{B}_{0.5\ \mathrm{M}}$	0.4	0.21	3.0	0.4	–	–	25	75	0.38	0.02
$\mathrm{B}_{1\ \mathrm{M}}$	–	–	6.0	0.55	–	–	18	75	0.38	0.02
$\mathrm{D}_{0.1\ \mathrm{M}}$	0.35	0.5	3.5	0.45	–	–	27	74	0.37	0.03
$\mathrm{D}_{0.5\ \mathrm{M}}$	0.35	0.5	3.2	0.4	–	–	28	75	0.38	0.03
$\mathrm{D}_{1\ \mathrm{M}}$	–	–	6.5	0.82	–	–	18	75	0.37	0.02
$\mathrm{E}_{0.1\ \mathrm{M}}$	0.4	0.15	1.0	0.4	–	–	25	75	0.38	0.02
$\mathrm{E}_{0.5\ \mathrm{M}}$	0.6	0.2	3.0	0.45	–	–	26	65	0.38	0.02
$\mathrm{E}_{1\ \mathrm{M}}$	–	–	6.0	0.8	–	–	10	70	0.42	0.02
$\mathrm{F}_{0.1\ \mathrm{M}}$	0.5	0.15	3.0	0.35	–	–	16	75	0.29	0.02
$\mathrm{F}_{0.5\ \mathrm{M}}$	0.5	0.18	2.0	0.4	–	–	15	75	0.38	0.02
$\mathrm{F}_{1\ \mathrm{M}}$	–	–	6.6	0.5	–	–	26	75	0.3	0.03

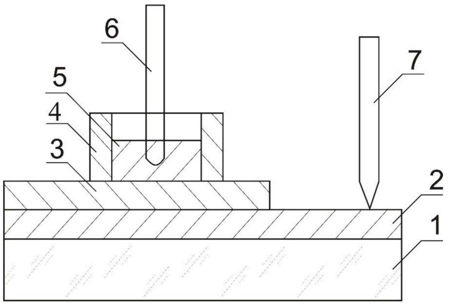

Fig. 2. Contacting device: 1 — sitallic substrate; 2 — aluminum film; 3 — anodic oxide film under study; 4 — fluoroplastic cylinder; 5 — drop of mercury; 6, 7 — measuring electrodes.

with no oxide film. If the position of the mercury electrode needed to be changed, the fluoroplastic cylinder with the mercury drop and the movable probe was being moved to the point with new coordinates.

The thickness of the oxide films was monitored with an MII-4 interferometer. Capacitance and dielectric losses were measured at 1000 Hz using the E7-25 impedance meter (Belarus). Breakdown voltages were measured using the UPU-5M unit (Russia). Specific capacitance was calculated as the quotient of the capacitance divided by the overlapping area of the capacitor claddings. Volumetric resistivity was measured according to the classical three-electrode scheme with aluminum claddings sputtering over the oxide.

3. Results and discussion

Figure 3 shows a qualitative dependence of the anode current i_{a} on ϕ_{a} for the background A-type electrolyte. Table I shows the values of the curve characteristic points. For the convenience of the curve analysis, the characteristic points of the dependence $i_{\mathrm{a}} = f(\phi_{\mathrm{a}})$ are introduced in Table I. As seen in Fig. 3, the $i_{\mathrm{a}} = f(\phi_{\mathrm{a}})$ dependence is characterized by several distinctive regions.

Similar dependences of the anode current i_{a} on the anode potential ϕ_{a} were obtained in electrolytes with other surfactant additives (electrolytes B–F). The range of anode potentials at which the anode current maintains a steady-state value is 10–80 V for all electrolytes (see Table I). Figure 4 shows a qualitative polarization curve for the electrolyte with the addition of ethylene glycol surfactant (electrolyte D). Table I gives values of characteristic points of the dependence of i_{a} on the anode potential for electrolytes B–F. The polarization curve for the A-type background electrolyte is given for comparison.

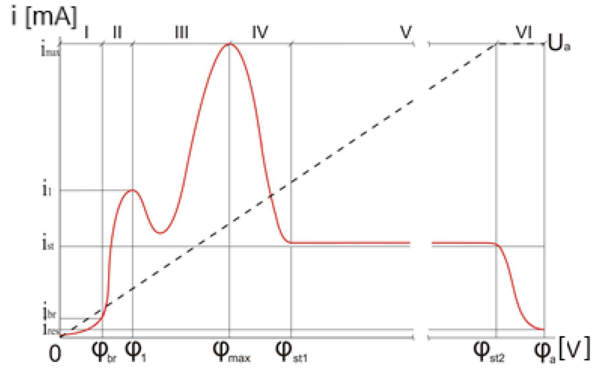

Fig. 3. Polarization curve during anodizing in 1% citric acid electrolyte. Here, the $i_{\mathrm{a}} = f(\phi_{\mathrm{a}})$ dependence is characterized by several distinctive regions: a region of small values of the anode current at potentials close to the steady state (I), a region of a sharp increase and peak current (II), a region that shows some decrease in the anode current with a further rise to maximum values (III), a region of a sharp decline in the current (IV), sections of constant current values, up to reaching the maximum forming potential (V), and a section of decline in the current at the potentiostatic anodization (VI).

As can be seen in Fig. 4a, the behavior of the dependence of $i_{\mathrm{a}} = f(\phi_{\mathrm{a}})$ in the background electrolyte differs significantly, qualitatively and quantitatively, from the data obtained previously when alcohols with a concentration of 0.1 M are introduced into the background electrolyte. A dependence identical to the dependence obtained in the A-type electrolyte is observed in the I region. As the voltage rises linearly, an electron current flows through the natural oxide. Then, at voltages from 0.3 to 0.7 V, an electrochemical breakdown of the natural oxide film and preferential growth of the anodic film in the defective sites of the natural oxide takes place. However, referring to Table I, the maximum values of currents in section II are 1.5–2 times lower than for anodizing in the background electrolyte. When the forming potential is further increased, there is no increase in the current (region III). The current level stabilizes after a certain decrease and becomes equal to the current observed during anodizing in the A-type electrolyte (regions III, IV, V). At the maximum anodizing voltage, the character and quantitative parameters of the anode current behavior in the potentiostatic mode also do not differ from those for the background electrolyte (section VI).

With an increase in the concentration of the additive to the background electrolyte by a factor of 5 (from 0.1 to 0.5 M), the behavior of the curves practically remains unchanged. Analysis of the $i_{\mathrm{a}} = f(\phi_{\mathrm{a}})$ dependence allows us to conclude that during the anodization in the electrolytes with alcohol additives up to a 0.5 M concentration, the surface is not activated, but inhibited.

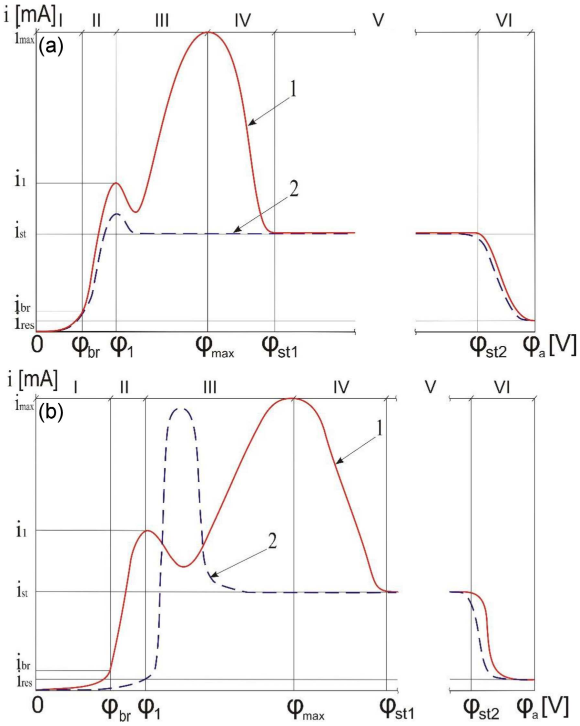

Fig. 4. Polarization curves in the electrolytes with surfactant additives: (a) surfactant concentration is 0.1–0.5 M; (b) surfactant concentration is 1 M.

When the surfactant concentration was increased to 1 M, we observed a significant difference in the curve behavior relative to anodizing both in the background electrolyte and in the electrolytes with low additive concentrations.

As the voltage begins to sweep linearly, no increase in the anode current is seen until $\phi_{\mathrm{a}} = 6$–7 V. This is followed by a sharp spike in the current, which has maximum values 1.2–2 times higher than for the background electrolyte. When the voltage is subsequently increased, the current through the oxide decreases and becomes 0.3–0.4 mA, which corresponds to similar values for the background electrolyte.

The chemical composition of the anodic aluminum oxide films was studied by the SIMS method. Figure 5 shows the secondary ion profiles for the samples obtained in the background electrolyte and in the electrolytes with the surfactant addition.

As can be seen in Fig. 5, the AlOH^{+} distribution profile along the thickness of the oxide film is $\sim$ 350 nm deep for the background electrolyte and $\sim$ 200 nm deep for the electrolyte with the surfactant addition. This can be attributed to the influence of negatively charged ions, primarily hydroxide ions injected into the oxide film from the electrolyte, as indicated by the increased yield of hydrogen-containing ions during sputtering (Fig. 5, curve 1). When the surfactant additive is introduced into the electrolyte, hydrogen-containing ions

TABLE II

Electrophysical properties of dense anodic alumina films

Film parameters	Electrolytes					
	A	B	C	D	E	F
bulk resistivity [Ω cm] ($\times 10^{-14}$)	5.2	5.2	6.7	7.3	5.8	7.4
specific capacity [μF/cm^2]	0.041	0.04	0.039	0.042	0.039	0.04
breakdown voltage [V]	64	69	66	70	70	68
dielectric loss tan(δ) ($\times 10^2$)	7–8	7–8	8	7–8	9	9

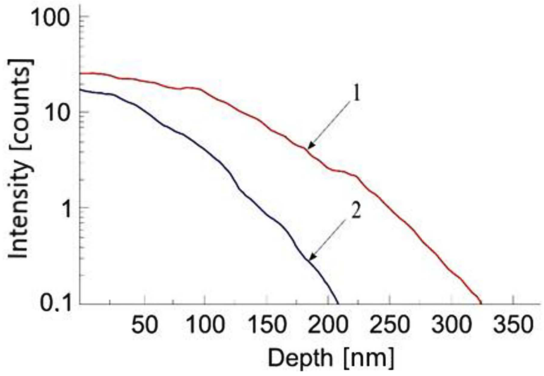

Fig. 5. SIMS-secondary ion profiles.

are localized at a narrow near-surface zone of the oxide film, and the secondary ions yield profile decreases significantly at the anodic alumina film thicknesses over 200 nm (Fig. 5, curve 2).

Comparing the obtained SIMS-analysis data with known ideas about the excess concentration of Al^{3+} ions in the oxide film at the metal-oxide interface and oxygen O^- ions at the electrolyte-oxide interface, we can assume that the anodic oxide formation with the stoichiometric composition of Al_2O_3 occurs more preferably under the surfactant inhibiting conditions of growing oxide surface than in the background electrolyte.

The structural composition of oxides obtained in different electrolytes should differ, especially at the electrolyte-oxide interface [6–7]. This should probably be the result of the protective effect of the surfactant molecules, preventing the penetration of electrolyte anions into the oxide. However, an excessive concentration of adsorbed molecules of organic compounds can lead to their incorporation into the bulk of the oxide film.

To verify the assumption about the influence of surfactant additives on the electrophysical properties of oxides, a comparative analysis of the basic dielectric properties of dense alumina films obtained in different electrolytes was performed. Referring to Table I, those are electrolyte A and electrolytes B–F with the concentration of 0.5 M. The anodizing voltage for all cases was 150 V. Table II illustrates the influence of surfactants on the dielectric properties of dense anodic alumina films.

As can be seen in Table II, the addition of surfactants to the anodizing electrolyte leads to an increase in the dielectric insulation resistance and breakdown voltage of the oxide films obtained. It is also indicated by the lower values of residual currents (21 instead of 32 mA) in the fabrication of dense aluminum oxide samples of the same thickness for SIMS analysis. When anodizing in electrolytes with surfactant additives, there is an insignificant decrease in the specific capacity of anodic alumina films, which can be explained by a decrease in the proportion of oxide with an increased concentration of hydroxyl groups on the outer surface of the oxide film. The dielectric losses in the films obtained in the electrolytes with surfactant additives practically do not differ from the similar characteristics of the samples anodized in the background electrolyte.

4. Conclusion

The research into the influence of the surfactant addition to the electrolytes for aluminum anodizing on the properties and composition of dense anodic alumina films obtained led to the following conclusions. The introduction of an alcoholic surfactant into the electrolyte for aluminum anodizing leads to the inhibition of the surface of growing oxide. The presence of surfactant molecules in the electrical double layer results in the formation of more stable Al_2O_3 films. The introduction of surfactants into the anodizing electrolytes leads to an improvement of the electrophysical properties of the obtained anodic alumina films.

References

[1] V. Surganov, A. Mozalev, *Microelectron. Eng.* **37–38**, 329 (1997).

[2] K. Watanabe, M. Sakairi, H. Takahashi, S. Hirai, S. Yamaguchi, *J. Electroanal. Chem.* **473**, 250 (1999).

[3] H. Uchi, T. Kanno, R.S. Alwitt, *J. Electrochem. Soc.* **148**, B17 (2001).

[4] X. Du, Y. Xu, *Thin Solid Films* **516**, 8436 (2008).

[5] T.N. Andryushchenko, A.E. Miller, US Patent US7560380B2, 2009.

[6] L. Schramm, E. Stasiuk, G. Marangoni, *Annu. Rep. Prog. Chem., Sect. C: Phys. Chem.* **99**, 3 (2003).

[7] M.J. Rosen, J.T. Kunjappu, *Surfactants and Interfacial Phenomena*, 4th Ed., John Wiley & Sons Ltd., New York 2012.

[8] L. Zaraska, G.D. Sulka, M. Jaskula, *Surf. Coat. Technol.* **204**, 1729 (2010).

[9] H. Kaur, L. Sharma, M. Kushwaha, *ECS J. Solid State Sci. Technol.* **5**, M154 (2016).

[10] C.M.A. Brett, A.M.O. Brett, *Electrochemistry: Principles, Methods, and Applications*, Oxford University Press, New York 1993.